ACS APPLIED MATERIALS & INTERFACES

www.acsami.org

Research Article

Fluorine-Free Extinguishing of a Hydrocarbon Pool Fire with a Suspension of Glass Bubbles Grafted with Nanoscale Polymer Layers

Randall T. Snipes, Mauricio Melara, Andrii Tiiara, Jeffery Owens, and Igor Luzinov*

Cite This: *ACS Appl. Mater. Interfaces* 2023, 15, 49749−49761

Read Online

ACCESS | Metrics & More | Article Recommendations | Supporting Information

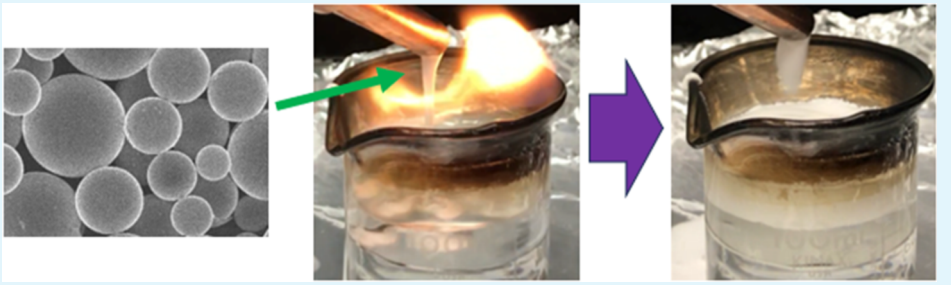

ABSTRACT: The current most efficient solution to extinguish liquid hydrocarbon (class B) pool fires involves fire-fighting foams containing fluorinated surfactants. However, fluorocarbon surfactants are unsafe due to their environmental persistence and negative toxicological/bioaccumulative impact. To this end, we show that fluorine-free aqueous suspensions of Glass Bubbles (GB) modified with hydrophilic polymer grafted layers can efficiently extinguish hydrocarbon pool fires. Namely, GB grafted with poly(oligo (ethylene glycol) methyl ether methacrylate) (POEGMA), GB-G was fabricated employing "grafting-through" and "grafting-from" methods and used to obtain the suspensions. It was found that the GB suspension, with a grafted layer of higher molecular weight and lower grafting density (GB-GL), proved superior to the more densely grafted GB-GH and nongrafted GB-0 system. The GB-GL suspensions displayed less negative spreading coefficients and viscosities lower than those of GB-GH/GB-0 compositions. When siloxane−polyoxyethylene surfactant was added to all GB suspensions, the interfacial properties were dominated by the surfactant, with all suspensions having the same positive spreading coefficient. However, the GB-GL-surfactant composition had the lowest viscosity among the suspensions studied in this work. Specifically, the viscosity of GB-GH and GB-0 suspensions at a shear rate of 77 s^{-1} was ∼110% and 70% higher than that of GB-GL. Due to the lower viscosity, the GB-GL suspension demonstrated the most efficient spreading over model hydrocarbon solid (polyethylene) and liquid (hexadecane) surfaces when the surfactant was added. The suspension also showed the best performance in the retardation of hexane evaporation when placed over the heated hexane pool. After 50 min, the amount of hexane that evaporated through GB-GH and GB-0 suspensions was ∼8 and 11 times higher, respectively, compared to the GB-GL suspension. We found that the GB-GL-surfactant system was the most efficient GB suspension in extinguishing the fire due to its superior spreading and sealing ability. It was within 10% of fluorine-containing foam's fire extinguishment performance. The GB suspensions are much safer in terms of burnback resistance as a torch applied directly to the suspension after extinguishment could not reignite the fire. The GB material is recyclable, since it can be collected and reused after application to a fire.

KEYWORDS: *firefighting, fluorine-free, glass bubbles, polymer grafted layer, polymer brushes, suspensions*

INTRODUCTION

The current most efficient solution to extinguish liquid hydrocarbon (Class B) pool fires involves firefighting foams containing fluorinated surfactants.[1] However, fluorocarbon surfactants are unsafe long-chain perfluoroalkyl substances (LCPFAs, C_nF_{2n+1}, $n \geq 7$), sometimes referred to as "forever chemicals"[2] in popular media due to their persistence in the environment and toxicological/bioaccumulative impact on humans and wildlife.[3−8] Significant efforts were undertaken to develop fluorine-free alternatives over the years.[9] Nevertheless, none of those fluorine-free foams extinguish a hydrocarbon pool fire as fast and efficiently as fluorocarbon-containing AFFFs (Aqueous Film Forming Foams).[9−15] The efficiency of AFFFs is based on the unique physicochemical properties of these foams that are considerably different from all of the other currently available firefighting compositions. Fluorinated surfactants of AFFFs lower the surface tension of

Received: July 13, 2023
Accepted: September 27, 2023
Published: October 10, 2023

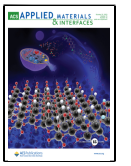

water to an unparalleled 16 mN m^{-1}, and the solution draining from the foam structure forms a continuous aqueous film on the surface of a volatile fuel, adding a barrier to fuel vapor diffusion to the burning fire.[16,17] It is also suggested that AFFF forms a significant barrier for fuel vapors because of the high foam stability arising from the oleophobicity of the fluorosurfactant.[18,19]

There are primarily two parameters essential to efficiently extinguishing a liquid fire: a firefighting agent should quickly spread across the liquid fuel, and after doing so, the foam layer should seal the fuel surface, blocking fuel vapor from oxygen above the foam.[17,19] For spreading to occur, the surface tension of the spreading medium and the interfacial tension between the spreading medium and the fuel surface should be low, as the spreading coefficient, SC (eq 1), should be positive for spreading to happen[20]

$$SC = \gamma_{A/F} - \gamma_{L/F} - \gamma_{A/L} \quad (1)$$

where $\gamma_{A/F}$ is the air−fuel interfacial tension, $\gamma_{L/F}$ is the interfacial tension between the spreading liquid and the fuel, and $\gamma_{A/L}$ is the air-spreading liquid interfacial tension. In addition to low surface and interfacial tension, the viscosity of the spreading medium should also be low.[21] When the density of the spreading medium is less than the density of the fuel, hydrostatic pressure acts on the spreading medium to flatten it across the fuel surface.[17] The viscosity of the spreading medium resists this flattening.[22] Therefore, the viscosity should be low to spread the material efficiently on the fuel efficiently.

Once the material has covered the fuel surface, the material's sealing property becomes very important. Hinnant et al. have argued that the ability of a foam structure to block fuel vapors from diffusing through the foam structure to the flame above the foam is the most important property in firefighting.[18,23,24] When fluorosurfactants, which have the unique advantage of having a tail that is both oleophobic and hydrophobic, are not used, no aqueous film is formed, and the prevention of fuel vapor diffusion depends primarily on the strength of the bulk foam structure. Fuel vapors attempt to degrade the foam structure, and as a rule, lower degradation and coarsening of the foam structure lead to lower fuel vapor diffusion through the foam. The strength of a foam structure in the presence of fuel vapors is dependent upon several interdependent factors, such as the rate of liquid drainage from the foam, which depends on the bulk viscosity and surface viscosity of the liquid, the latter of which increases with an increasing packing density of the surfactant at the air−water interface.[17] Additionally, as fuel water solubility increases, fuel vapor diffusion through the foam increases.[25] Fluorine-free surfactants, unlike fluorosurfactants, lack an oleophobic tail. For this reason, fuels are more soluble in fluorine-free foams than in fluorinated foams. Therefore, the cells of nonfluorinated foams usually contain fuel vapors and air, which is a mixture that can ignite given enough heat.[17]

Hence, the major barriers to developing nonfluorinated foams having the same efficiency as AFFFs are the higher surface tension of nonfluorinated surfactants and the affinity of their hydrophobic block to the hydrocarbon liquids. Those fundamental challenges cannot be overcome with any known nonfluorinated substances. To this end, we aimed to beat this "physicochemical impossibility" by generating a physical water-containing barrier, preventing the hydrocarbon fuel evaporation during a fire. Our design used commercially available low-density hollow glass bubbles (GB) modified with "water-holding" hydrophilic poly(oligo (ethylene glycol) methyl ether methacrylate) (POEGMA) grafted layers, GB-G. In fact, a water suspension of GB-G (containing an environmentally friendly siloxane surfactant), placed on the pool of liquid hydrocarbon, quickly spreads over and practically arrests the fuel evaporation. We found that increasing the molecular weight and decreasing the graft density leads to a larger water shell surrounding the GB-G, lower suspension viscosity, increased spreading of the GB-G layer across a hydrophobic surface, and better sealing of the hydrocarbon liquid surface. These properties contribute to the significant firefighting performance of the suspension composed of GB-G. This suspension is within 10% of the fire extinguishing efficiency of an industrial AFFF, yet our environmentally friendly firefighting composition is much safer in terms of burnback resistance, as a torch applied directly to the suspension after extinguishment could not reignite the fire. Finally, our material can be collected and reused after application to a fire, which is a capability that no liquid foam or dry chemical possesses.

EXPERIMENTAL SECTION

A detailed description of experimental procedures is presented in Supporting Information (S2).

Materials. The following materials were used in this study: S32HS GBs (3M) glass bubbles provided by 3M; methyl ethyl ketone (MEK) [Fisher, technical grade]; 3-(trimethoxysilyl) propyl methacrylate (TMSPM) [98%, Sigma-Aldrich]; oligo(ethylene glycol)methyl ether methacrylate (OEGMA) [M_n 300 g/mol, Sigma-Aldrich]; monomethyl ether hydroquinone (MEHQ) and *tert*-butylcatechol inhibitor removers [Sigma-Aldrich], azobis(isobutyronitrile) (AIBN) [Sigma-Aldrich]; toluene [HPLC grade, Alfa Aesar]; (3-glycidyloxypropyl)-trimethoxysilane (GPS) [Sigma-Aldrich]; dimethyl sulfoxide (DMSO) [99.7%, Thermo Scientific]; 4,4′-azobis (4-cyanovaleric acid) (ACP) [Sigma-Aldrich]; 2-methylpyridine [98%, Sigma-Aldrich]; AFFF [Solberg Arctic AFFF 6% concentrate]; hexadecane [99%, Sigma-Aldrich]; diethylene glycol monobutyl ether (DGBE) [Sigma-Aldrich]; DOWSIL 502W (provided by DOW Chemical); and Glucopon 225DK (provided by BASF).

Modification of GBs with Polymer Grafting. To obtain GB-GL ("grafting through" method,[26] SI: Figure S1), the GBs were first modified with TMSPM. Next, OEGMA was grafted to the surface employing double bonds of TMSPM by the solution radical polymerization initiated by AIBN. For the synthesis of GB-GH ("grafting from" method,[27] Figure S2), the GB surface was modified with GPS and then with the attachment of initiator (ACP) via the epoxy groups of GPS. OEGMA was grafted to the GB surface by solution radical polymerization initiated by AIBN in the solution and ACP from the surface. The obtained GB-GL and GB-GH glass bubbles were rinsed three times with MEK to remove the ungrafted polymer and dried.

Characterization. Scanning electron microscopy (SEM) was performed on a Hitachi SU9000. Thermogravimetric analysis (TGA) was conducted using a TA Instruments AutoTGA 2950 instrument using a 20 °C/min temperature ramp rate up to 600 °C. The weight-average molecular weight (M_w) was determined using dynamic light scattering (DLS) (Malvern Instruments Zetasizer Nano ZS) and static light scattering (SLS) with a Brookhaven BI-200SM Goniometer in combination with a 640 nm HeNe laser (45 mW). To measure the surface tension, the pendant drop method was used [Krüss Drop Shape Analyzer (DSA10)]. An inverted needle was placed into a hexadecane pool for the interfacial tension measurements, and the pendant drop was analyzed by using the DSA software. The viscosity experiments used a Brookfield Ametek DV3THBCJ viscometer (spindle CP-42). The UV−vis spectra were obtained with a Shimadzu UV3600 UV−vis−NIR Spectrophotometer. Fire temperature was measured using FLIR TG165 Imaging IR Thermometer. An infrared hexane gas sensor (ATI D12Ex-IR transmitter with a 00-1905 sensor)

https://doi.org/10.1021/acsami.3c10228
ACS Appl. Mater. Interfaces 2023, 15, 49749−49761

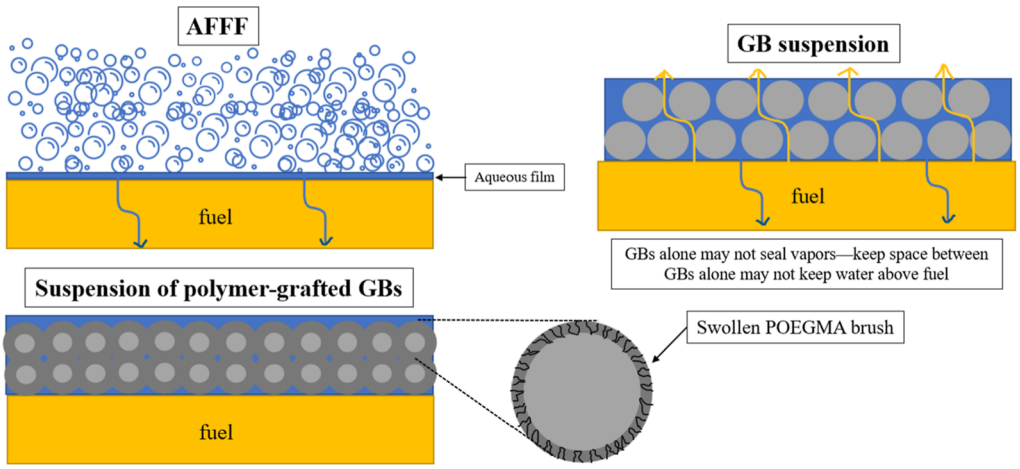

Figure 1. Summary of our approach in this work. AFFF forms a water film over the fuel, which aids in sealing the fuel surface. GBs are light and float on fuel, but without modification, a suspension of GBs does not sufficiently hold water above fuel. If modified with a hydrophilic polymer brush, the GBs swell with and hold water above the fuel surface, which seals the fuel surface, like AFFF does with an aqueous film. The parameters of the polymer brush layer significantly affect the properties of the overall suspension.

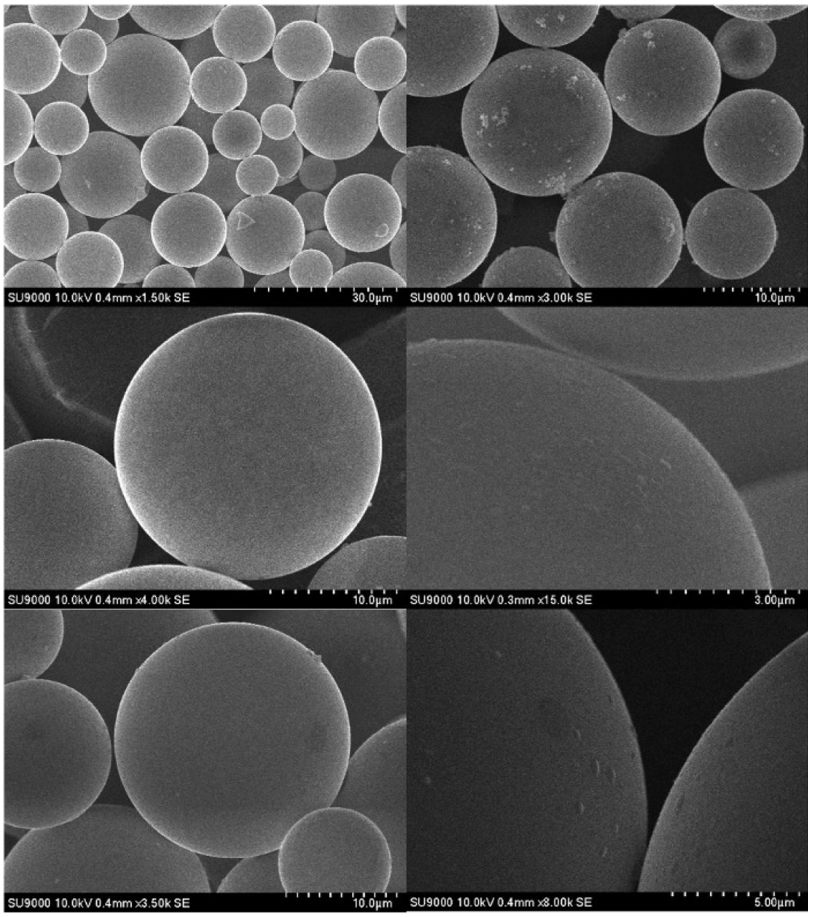

Figure 2. SEM images of (top) GB-0, (middle) GB-GL, and (bottom) GB-GH.

was used to determine the level of hexane evaporation. A humidity sensor (Omega HX71-MA) was employed to measure water evaporation.

RESULTS AND DISCUSSION

Approach. Our approach is summarized schematically in Figure 1. Considering the aforementioned critical parameters, we targeted a fluorine-free firefighting composition that could spread quickly across and hold water above the fuel surface without degradation by the vapors. Glass bubbles were selected because of their low density and low thermal conductivity.[28] We established that dry GBs wick fuel; therefore, the GBs have to be applied to a fuel surface as an aqueous suspension. However, we envisioned that the GBs should be modified with a hydrophilic polymer shell to create a gel-like water-holding outer shell when the GBs are dispersed in water. Doing so

https://doi.org/10.1021/acsami.3c10228
ACS Appl. Mater. Interfaces 2023, 15, 49749−49761

Table 1. GB Polymer Grafting Data and Calculations

parameter	GB-GL	GB-GH
POEGMA grafted (wt %)	0.8	1.8
effective M_w $\times 10^{-5}$ (g/mol)	3.5	1.1
effective N	1167	353
$\langle r^2 \rangle^{1/2}$ (nm)	68	33
t_d (nm)	6	13
σ (chains/nm^2)	0.01	0.07
D (nm)	11	4
t_s (nm)	295	90
f_w	0.98	0.88
%, free water in suspension	81	94
EF	6.1	8

Table 2. Surface Tension (ST), Interfacial Tension (IFT), and Spreading Coefficient (SC) Data

material	ST (mN/m)	IFT with hexadecane (mN/m)	SC on hexadecane (mN/m)
H_2O	72.8 ± 0.5	50.6 ± 0.5	−97 ± 1
siloxane	22.1 ± 0.2	2.8 ± 0	2.1 ± 0.2
AFFF	16.5 ± 2.5	2.7 ± 0	7.7 ± 2.5
GB-0	64.7 ± 1.2	39.4 ± 0.4	−77 ± 1.6
GB-GL	52.9 ± 1.4	21.4 ± 1.8	−47 ± 3.2
GB-GH	57.8 ± 1.3	19.9 ± 0.4	−51 ± 1.7
GB-0-s	21.8 ± 1.1	2.7 ± 0.2	2.4 ± 1.3
GB-GL-s	21.8 ± 1.1	2.7 ± 0.2	2.4 ± 1.3
GB-GH-s	21.8 ± 1.1	2.7 ± 0.2	2.4 ± 1.3

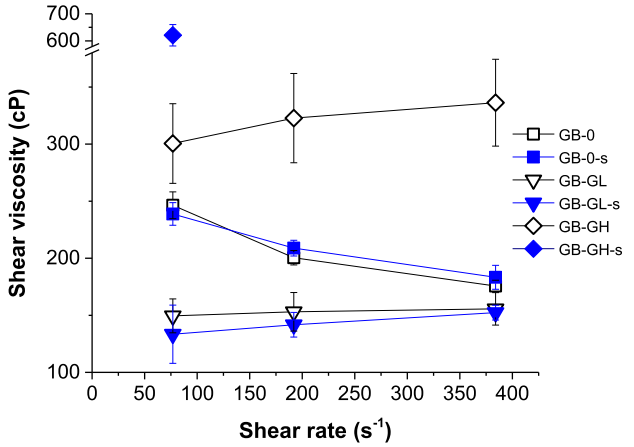

Figure 3. Shear viscosities of the GB suspensions as a function of the applied shear rate. The GB-GH-s suspension went over the cone of the rheometer at the higher shear rates due to its high viscosity, therefore the measurements at these rates are invalid and not included.

increases the amount of water held above the fuel by the suspension, which aids in sealing the fuel surface. Additionally, it was assumed that lubrication between GBs provided by the swollen water-grafted layer could decrease the viscosity of the suspension, aiding the spreading. We fabricated two different types of polymer-modified GBs≡one with long, sparsely grafted chains of a brush-like polymer and the other with short, densely grafted chains of the same brush-like polymer to observe the effect of grafted layer structure on the firefighting performance of GB-G suspensions.

Glass Bubbles Used in This Study. In this work, we used commercially available glass bubbles with a reported density of

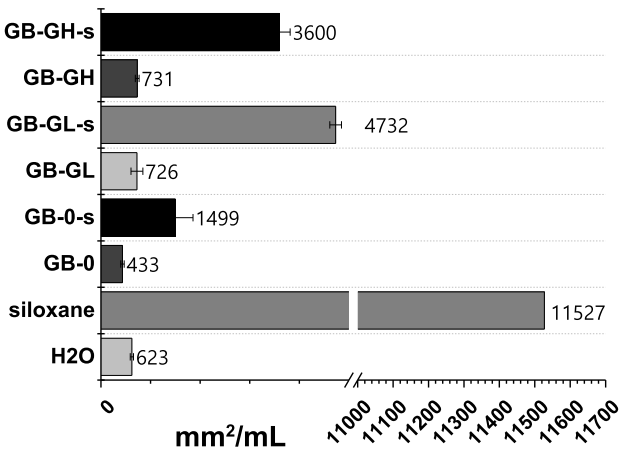

Figure 4. Spreading values (mm^2/mL) for GB suspensions, siloxane solution, and water on polyethylene.

0.32 g/cm^3. The scanning electron microscopy (SEM) images of the GBs are shown in Figure 2. The image analysis of ∼200 bubbles found that the average diameter of the GB in the batch used here was 13.4 μm (Table S1 and Figure S3). The small agglomerates on the surface of the unmodified GBs are the anticaking agents used by the manufacturer.

Using two free radical grafting techniques, we anchored POEGMA with ∼5 ethylene glycol units per monomeric unit to the GBs at different grafting densities. For the GBs with a lower grafting density (GB-GL), a "grafting-through" method was used.[26] To fabricate a densely grafted POEGMA layer on the GBs (GB-GH), we employed a "grafting-from method.[27] In the "grafting through" method, first, a methacrylate group was attached to the GBs via silane coupling, and then polymerization occurred through the double bonds of methacrylate groups on the surface (Figure S1). In the "grafting-from" method, an epoxy group was attached via silane coupling to the GB surface, then an initiator group was tethered through the reaction of the epoxy group on the surface with the carboxylic acid group present in the initiator molecule (Figure S2). Using the initiator-functionalized GBs, we polymerized the GBs from the surface. Experimental details of the grafting are presented in S2.1.

The SEM imaging of the GBs grafted with the polymer layers indicated that grafted POEGMA forms a homogeneous layer evenly covering the surface of the glass bubbles (Figure 2). Therefore, the grafted layer was considered to be a uniform shell enveloping GBs. In calculations of the grafted layer parameters (Table 1), the molecular weight of the grafted macromolecules was assumed to be the same as the one formed in the solution.[29−31] Thus, after the grafting was complete, we measured the weight-average molecular weight of the polymer formed in the solution via static light scattering (SLS), S2.3. Thermogravimetric analysis (TGA) was performed on the GBs to determine the amount of polymer grafted, and the dry thickness of the polymer layer was calculated by assuming a homogeneous polymer shell. Then, the graft density (σ) and distance between grafting sites (D) (Table 1) were calculated from the molecular weight and polymer layer thickness (eqs S2 and S3).[32] For GB-GL, since the polymer was grafted through a monomer attached to the GB surface, the molecular weight of each chain protruding from the surface is accepted to be half the molecular weight of the polymer chain in solution.

https://doi.org/10.1021/acsami.3c10228
ACS Appl. Mater. Interfaces 2023, 15, 49749−49761

Figure 5. Examples of droplets of GB suspensions on hexadecane: GB-0 ellipsoid (left), GB-0-s half ellipsoid (middle), and GB-GH-s ellipsoid (right).

Table 3. Droplet Placed on the Hexadecane Pool Behavior Summary

system	droplet behavior on hexadecane
siloxane	complete spread
GB-0, GB-GL, GB-GH	ellipsoid formation
GB-0-s	lens formation
GB-GL-s	complete spread
GB-GH-s	ellipsoid formation

We estimated the amount of water that could be incorporated into the grafted polymer layer upon swelling. First, based on the degree of polymerization of the chains grafted, we calculated the root-mean-squared end-to-end distance of the grafted macromolecule in the aqueous environment, $\langle r^2 \rangle^{1/2}$. It was determined as AN^d, where A is the statistical segment length (assumed to be typical for methacrylates 0.65), N is the degree of polymerization, and d is equal to 0.6 (water is a very good solvent for POEGMA), Table 1.[33−35] One can see that the end-to-end distance is significantly smaller than the distance between the grafted sites. Therefore, the grafted layer is in a brush regime, where the anchored macromolecules stretch away from the surface to avoid crowding.[36−39] We used the formula for the height of a polymer brush swollen in a good solvent to estimate the brush height of GB-GL and GB-GH in water (eq S4).[36] For both GB-GL and GB-GH, the swollen height calculated was greater than the length of the fully extended polymer chain (eq S5). We associate this finding with the specific chemical structure of the POEGMA macromolecules having relatively long side moieties. Thus, the macromolecules cannot be considered classical linear homopolymers but rather as having a molecular brush structure, where relatively long side chains are anchored to the backbone at high grafting densities.[40−44] Molecular bottlebrushes typically have relatively high chain stiffness due to excluded volume effects[40−42,45,46] and, therefore, can extend beyond the typical values theoretically predicted for the linear chains. Therefore, the fully extended length of the polymer chain (eq S5) was used as the swollen height of the grafted layer. Using the brush height, we estimated the fraction of water incorporated in the polymer shell, which is as follows:

$$f_w = 1 - \left(\frac{t_d}{t_s}\right) \tag{2}$$

where f_w is the fraction of water in the shell, t_d is the dry thickness of the polymer shell, and t_s is the swollen thickness of the polymer shell.

All glass bubble suspensions used in this study were prepared at the same concentration: 30 wt % in water. This concentration was used because it is slightly (5%) below the maximum flowable GB concentration, and we wanted the suspension to have the lowest density possible (Figure S5).[47] We calculated the percent of free water in each polymer-modified GB suspension (eq S6) based on the swollen size of the polymer shell and the concentration of GBs in suspension (Table 1). Finally, we calculated the "extension factor" (EF) of the grafted polymer in water (Table 1) according to the following equation:

$$\mathrm{EF} = \frac{\langle r^2 \rangle^{1/2}}{D} \tag{3}$$

Spreading Coefficient of the Glass Bubble Suspensions. To calculate the spreading coefficient, which indicates the GB suspension's thermodynamic tendency to spread over a liquid hydrocarbon pool, we experimentally determined the

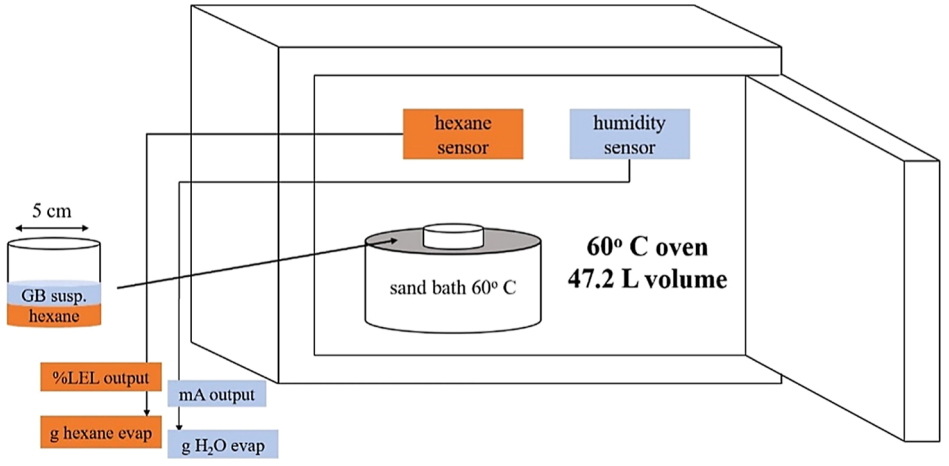

Figure 6. Sealing experiment schematic.

https://doi.org/10.1021/acsami.3c10228
ACS Appl. Mater. Interfaces 2023, 15, 49749−49761

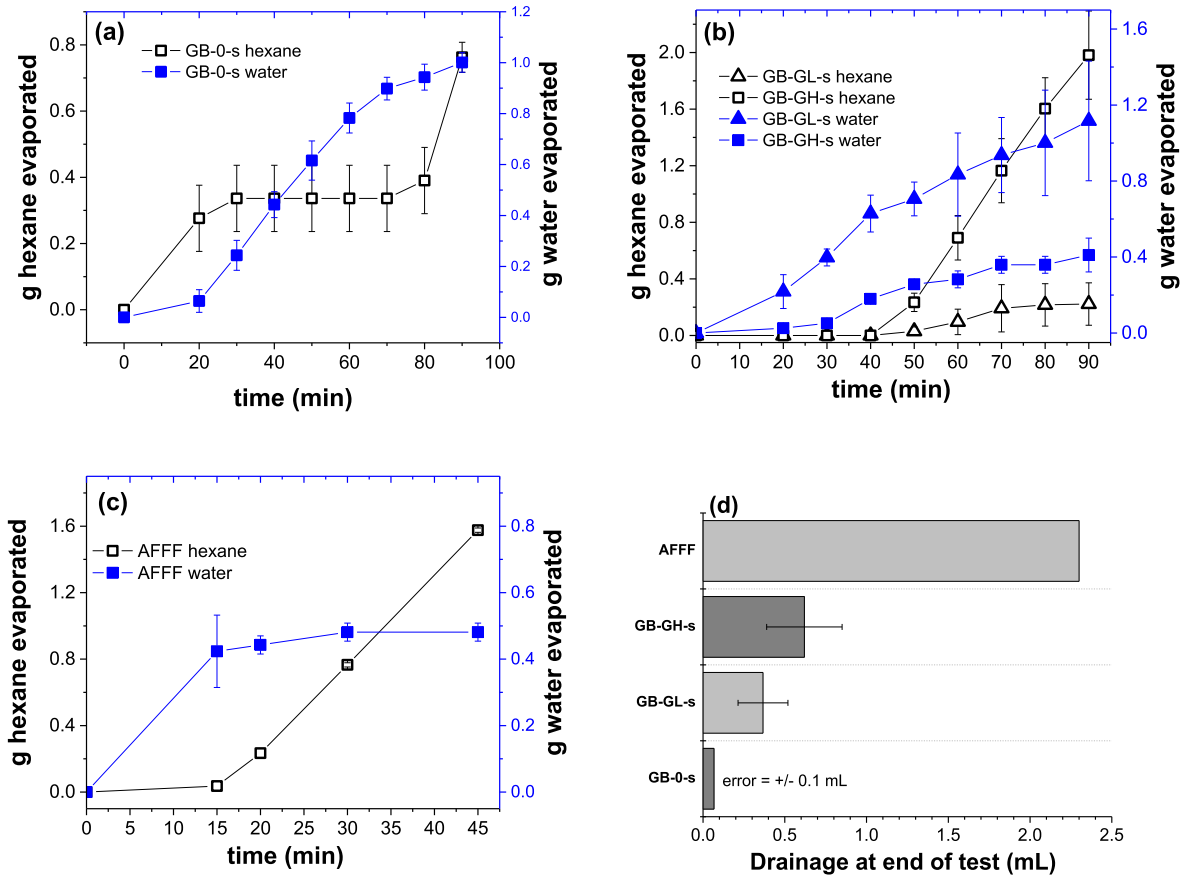

(e)

Material	Hexane evaporation @ 90 min. (g)	H_2O evaporation @ 90 min. (g)
GB-0-s	0.76 ± 0.05	1.00 ± 0.04
GB-GL-s	0.22 ± 0.15	1.12 ± 0.31
GB-GH-s	1.98 ± 0.31	0.41 ± 0.09
AFFF	3.76 ± 0	0.48 ± 0.03

Figure 7. Sealing experiment results. Hexane and water evaporation over time for (a) GB-0-s, (b) GB-GL-s and GB-GH-s, and (c) AFFF (note the time scale is 45 min). (d) Water drainage of each system at the end of the test (90 min). (e) The total hexane and water evaporation of each system after 90 min.

surface energies and interfacial tensions for the GB water suspensions (Table 2). All measurements were made using the pendant drop method (S2.5). Hexadecane was used as a model liquid hydrocarbon for interfacial tension measurements. We also measured the surface and interfacial tensions for water and AFFF (6%) solution to confirm the accuracy of our measurements (Table 2). The obtained results were close to those reported in the scientific literature.[48] The data in Table 2 show that unmodified glass bubbles (GB-0) slightly reduced the aqueous suspension's surface and interfacial tension to values approximately 10 mN/m lower than that of water. This result indicates that GB-0 bubbles migrate to the surface and interface with the liquid hydrocarbon to reduce the surface/interfacial tension. However, the spreading coefficient (Table 2) for the GB-0 suspension is strongly negative. Thus, the GB-0 suspension, from a thermodynamic point of view, cannot spread over the hydrocarbon pool surface.

When the glass bubbles are grafted with POEGMA macromolecules, the suspension surface and interfacial tension are reduced to values significantly lower than those found for water and the GB-0 suspension. The interfacial tension with hexadecane of the GB-GL and GB-GH suspensions was roughly half that of GB-0 (Table 2). This observation implies that even though the polymer shell contains mostly water, the polymer segments with lower surface energy dominate the surface and interface. This can be expected since even the grafted POEGMA brush is hydrophilic; POEGMA macromolecules contain hydrophobic methacrylate, $-CH_2-$ and initiator end-groups, presented at the surface/interface. Nevertheless, the spreading coefficient for the aqueous suspension of the bubbles modified with the polymer shell remains highly positive, suggesting no spontaneous GB-G suspension spreading will occur on a liquid hydrocarbon.

To decrease surface/interfacial tensions of the suspensions, siloxane-polyoxyethylene surfactant (further called "siloxane"), having the chemical structure shown in Figure S6, was added to the suspensions. Those compositions contained 30 wt % GBs in a 0.3% siloxane aqueous solution and are labeled here

https://doi.org/10.1021/acsami.3c10228
ACS Appl. Mater. Interfaces 2023, 15, 49749−49761

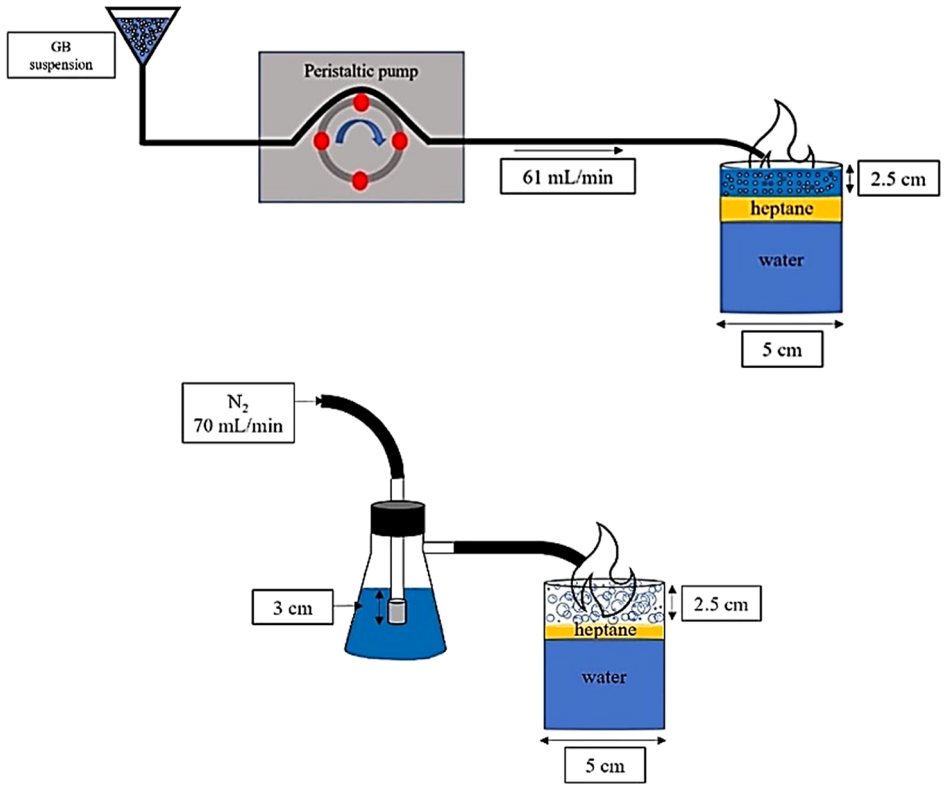

Figure 8. Fire extinguishment experiment schematic: (top) setup for suspensions and (bottom) setup for foams. In the suspension setup, we made the heptane pool deeper to avoid the suspensions touching water when applied.

as "GB-(0, GL, or GH)-s". This siloxane concentration is approximately 5 times the surfactant's critical micelle concentration (CMC) and is equivalent to the siloxane concentration used by researchers from US Naval Research Laboratory (NRL) to formulate quite effective fluorine-free firefighting foams.[9,18,19,23−25,49] Prior to forming the compositions, we measured the surface and interfacial tension of the siloxane solution and determined that it is 22.1 and 2.8 mN/m, which is close to the values reported elsewhere.[50] For GB-based compositions containing siloxane, it was found that the surfactant dictates the surface and interfacial properties of the suspensions as their surface and interfacial tensions are identical to those of the siloxane solution (Table 2). It is noted that the spreading coefficients for the siloxane solution and the siloxane-containing suspensions are positive. So, we can expect the spreading of those suspensions over the hydrocarbon surfaces.

Viscosity of the Glass Bubble Suspensions. Since firefighting is a dynamic process in addition to a high spreading coefficient, the viscosity of the spreading medium has to be low to spread the material on the fuel efficiently. To this end, using cone and plate rheometers, we measured the shear viscosity of the GB suspensions at shear rates of 77, 192, and 384 s^{-1}. This method was used because the cone's movement effectively mixes the suspension as the measurement is conducted, and GB-water separation is avoided. We note that all suspensions we studied here demonstrate regular behavior observed for concentrated suspensions of hard spheres, where the suspension behaves as a solid until a critical yield stress is applied.[51] It is established[52] that suspensions of hard spheres typically exhibit a three-phase rheological pattern. The suspensions demonstrate nearly constant viscosity at lower shear rates (equilibrium state), then exhibit shear thinning at intermediate shear rates, and finally enter a shear thickening regime, plateauing at the highest rates. In the equilibrium regime, the particles are randomly dispersed in liquid media. The particles form chainlike structures aligned in the shear direction in the shear-thinning regime. Shear thickening originates from hydroclusters forming, which inhibit flow.

By measuring the viscosity of the suspensions at multiple shear rates, it was found that GB-GL and GB-GH compositions exhibited nearly constant viscosity behavior (within the experimental error), whereas the GB-0 material displayed shear thinning behavior (Figure 3). Therefore, the GB-0 suspension is within the second shear-thinning regime for the shear rates used. The viscosity of GB-GL is lower than that of GB-0 but not decreasing/increasing, which indicates the random distribution of the particles in the dispersion. This originates from the water-swollen polymer brush layer around the GB-GL particles providing lubrication and repulsion between particles.[53,54] Conversely, the GB-GH composition has a much higher viscosity than GB-0 and GB-GL ones yet demonstrates nearly constant viscosity over the share rates used here. There are two possible scenarios for the trend observed: (1) the GB-GH suspension is in the equilibrium regime or (2) the suspension is in the shear-thickening plateau region, where the hydroclusters are forming. The limited data collected in this study do not allow us to differentiate between the two scenarios above. We associate the considerable increase in the viscosity with attractive hydrophobic interactions[54] between hydrophobic initiator end-groups located on the grafted macromolecules terminated via the recombination mechanism. Indeed, since the densely grafted POEGMA chains are highly extended, a significant number of the end groups become exposed at the exterior of the grafted layer

https://doi.org/10.1021/acsami.3c10228
ACS Appl. Mater. Interfaces 2023, 15, 49749−49761

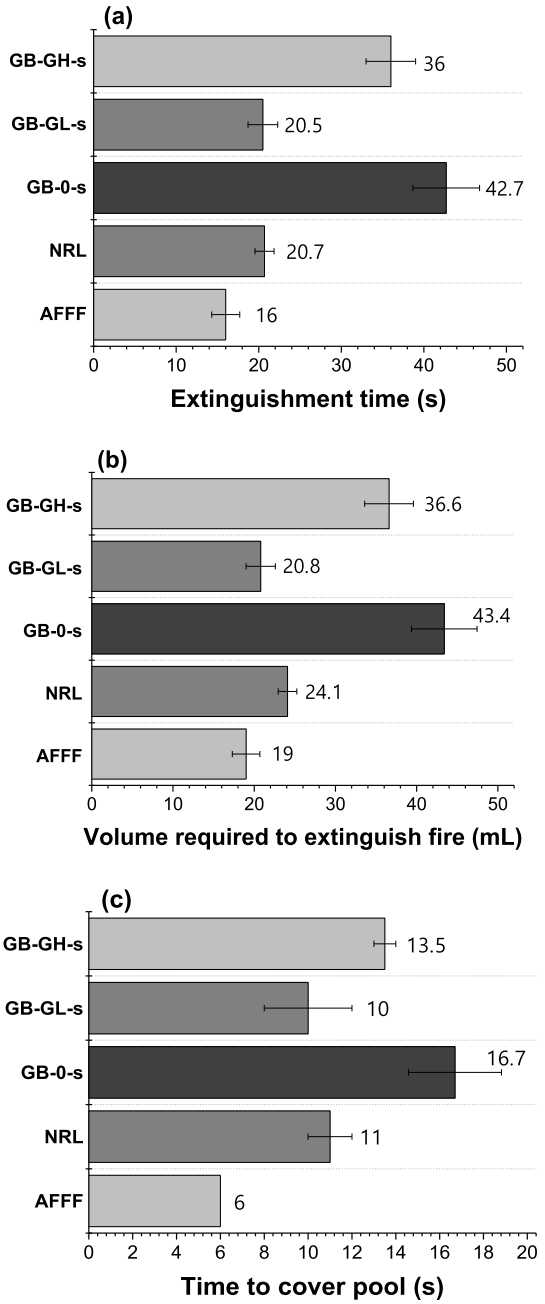

Figure 9. (a) Fire extinguishment times, (b) volume of each material required to extinguish the fire, and (c) time required to cover the heptane surface for each material.

exterior. As a result, the level of contact attraction between the glass bubbles increases, triggering a viscosity increase.

It is observed that the addition of siloxane to GB-0 and GB-GL suspensions does not change the viscosity within the experimental error of our measurements. However, qualitatively, the viscosity of the GB-0-s and GB-GL-s compositions tends to decrease slightly with surfactant addition. We associate this viscosity decrease to additional lubrication between the glass bubbles and the hydrated corona of the surfactant aggregates. Indeed, according to Soni et al.,[55] the micellar aggregates for polyoxyethylene-modified poly(dimethylsiloxane) have an ellipsoid shape with hydrophilic polyoxyethylene corona. The aggregates (with dimensions independent of concentration) have major and minor axes equal to ∼10 and 5 nm, respectively. Unexpectedly, the GB-GH-s composition doubled in viscosity compared with GB-GH, Figure 3. We could measure the viscosity only at the lowest rate used for this suspension. For the higher rates, the GB-GH-s suspension went over the cone of the rheometer due to its high viscosity. This is surprising since the micelles' corona is composed of hydrated polyoxyethylene moieties that sterically repel the hydrated OEGMA units of a similar structure. To comprehend this finding, we suggested that the densely grafted polymer brush mostly rejects penetration of the surfactant micelles into the swollen grafted layer. As a result, the concentration of micelles in the "free" water in the interparticle space rises, considerably increasing its viscosity.[55] Correspondingly, the viscosity of the suspension increases significantly.[51,56] In fact, the distance between grafting sites for the GB-GL suspension (no significant change in viscosity with the siloxane addition) is comparable to the aggregate dimensions, while for the GB-GH suspension, the distance is considerably lower than that (Table 1). So, the probability of rejection is much higher for the GB-GH material.

To evaluate the scenario above, we conducted a UV−vis experiment wherein the surfactant concentration in the aqueous drainage from the glass bubbles was measured (S2.8, Figure S7). It was found that GB-0-s particles adsorbed the surfactant on the surface since the siloxane concentration in the drainage was somewhat lower than that in the initial solution. Specifically, it decreased from 0.33 to 0.21%. For GB-GL-s, we observed a small (from 0.33 to 0.4%) increase in the surfactant concentration, indicating low-level rejection of the aggregates by the grafted layer. For GB-GH-s, however, significant rejection of siloxane was found, where the concentration increased to 0.67%. Thus, the increase in the suspension viscosity for GB-GH-s particles covered with the densely grafted layer can be associated with an increased surfactant concentration in the water located in the interparticle space.

Spreading of GB-Based Suspensions on Model Solid Hydrocarbon Surface. We measured the spreading of the GB suspensions, water, and siloxane solution on polyethylene plates to correlate the spreading pattern with the spreading coefficient and viscosity of the suspensions. We employed polyethylene because it is a hydrophobic solid surface with a surface tension (∼35 mN/m) comparable to that of heptane (∼20 mN/m) or cyclohexane (∼25 mN/m).[57−59] The solid surface was initially used to avoid complications from the suspension's ability to penetrate the hydrocarbon liquid. In our experiment, we placed a polyethylene sheet on a balance with a camera directly above the sheet. Then, a droplet of suspension was placed onto the surface using a disposable pipet, its weight was recorded, and a photo was taken of the droplet once it reached equilibrium on the surface. We calculated the droplet volume (with the recorded mass and known density) and measured the area the droplet spread over from a recorded image. The results of the measurements are reported in mm^2/mL (Figure 4), with a higher value indicating better spreading.

It is apparent that a combination of surface/interfacial tension and viscosity plays a role in droplet spreading. For example, water has a higher surface tension than GB-0 (Table 2), yet water's spreading value was larger. This can be attributed to the high viscosity of GB-0, which provides resistance to spreading. This trend is also evident in a comparison of GB-0 and GB-GL/GB-GH suspensions. GB-GL and GB-GH with surface/interfacial tensions lower than that of

https://doi.org/10.1021/acsami.3c10228
ACS Appl. Mater. Interfaces 2023, 15, 49749−49761

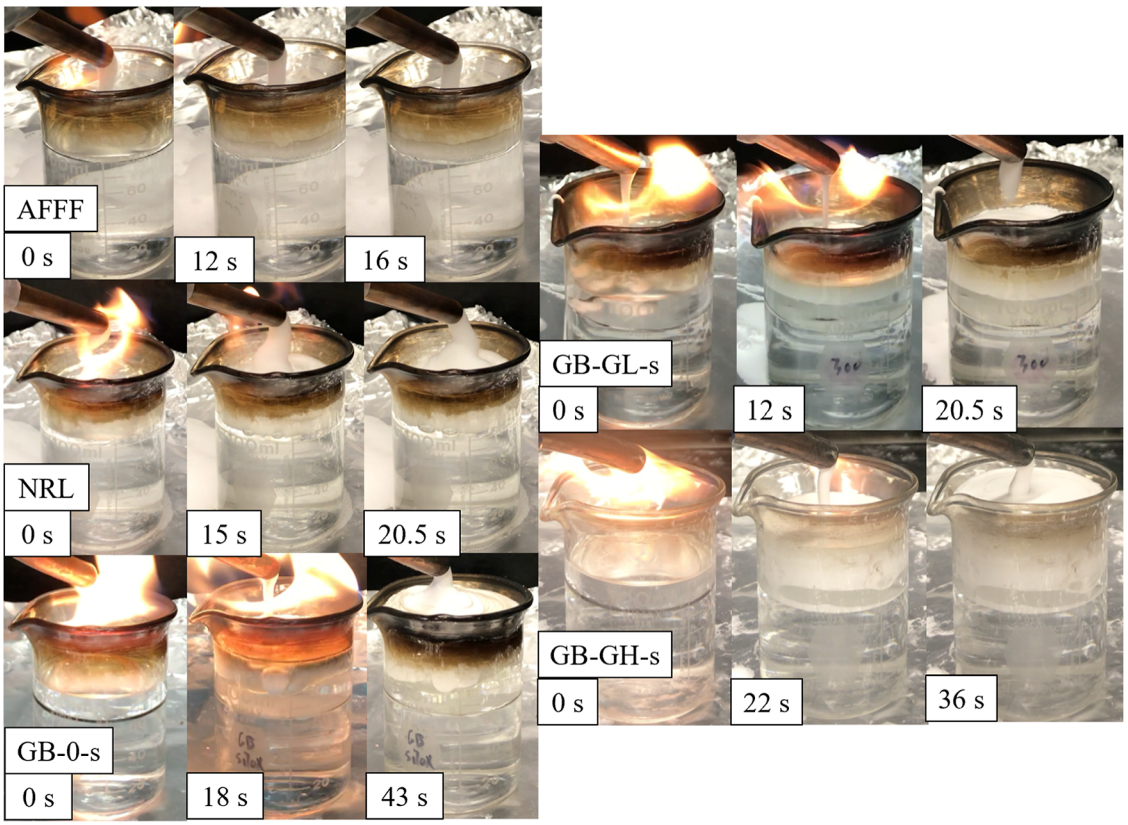

Figure 10. Frames during the firefighting extinguishment test for materials of interest.

GB-0/water demonstrate better spreading, irrespective of their viscosity. When siloxane is added to the suspensions, the surface/interfacial tensions and spreading coefficients are identical for all compositions and have the same value as the surfactant solution (Table 2). All GB suspensions spread to a significantly lower degree than the surfactant solution without glass bubbles (Figure 5). However, GB-GL-s spread ~3 times more than GB-0-s, presumably due to its lower viscosity. For GB-GH-s, the spreading value reported is not fully accurate since, when the very viscous suspension was placed on the surface, some GB-GH bubbles stayed in the pipet. Therefore, the concentration of this composition was reduced. Nevertheless, the spreading value for GB-GH-s was lower than GB-GL-s, presumably due to the higher viscosity of GB-GH-s. Generally, the low viscosity and low surface/interfacial tension GB-GL-s suspension demonstrates the best spreading on the polyethylene surface among all glass bubble compositions.

Spreading of GB-Based Suspensions on Model Liquid Hydrocarbon Surface. We also measured the spreading of the suspensions on the hexadecane pool. Hexadecane was selected because of its low volatility and surface tension (~28 mN/m).[58] In this experiment, a droplet of each suspension from a pipet in a fixed position was placed onto a cuvette filled with the liquid. Videos of those experiments are posted Videos S1–S5. Three different phenomena were observed: ellipse formation, half-ellipse formation, and complete spreading (Figure 5 and Table 3). First, we observed complete and rapid spreading for the siloxane solution (no GBs), which has a positive spreading coefficient and low viscosity. The GB-0 suspension formed a floating ellipsoid on the surface of the hexadecane as the spreading coefficient for this system is −77 mN/m. The GB-GL and GB-GH suspensions also formed ellipsoids similar to those of GB-0, as their spreading coefficients are −47 and −51 mN/m, respectively. GB-0-s formed a half ellipsoid or lens on the hexadecane surface because, even though the spreading coefficient is 2, its high viscosity prevented the suspension from fully spreading. GB-GL-s completely spread over the hexadecane surface, as the spreading coefficient is also 2, but its viscosity is low enough to enable complete spreading. For GB-GH-s, because of its high viscosity, we did not use a pipet (to avoid clogging). Instead, we used a small spatula to scoop the suspension into the hexadecane pool. We found that the GB-GH-s suspension did not fully spread over the hexadecane surface, presumably due to its high viscosity. Our results indicate that in terms of spreading, the GB-GL-s suspension has the highest potential to be employed for fluorine-free extinguishing of a hydrocarbon pool fire.

Sealing Ability of the Glass Bubble Suspensions. Once the suspension has spread over the pool surface, it must suppress the permeation of hydrocarbon vapors through the suspension for effective fire extinguishment. To measure the sealing ability of the GB suspensions, we developed a system where we can measure, in a heated environment, hydrocarbon vapor flux through a foam or suspension as well as water evaporation from the foam or suspension. A typical test run for 90 min, and the total volume of water drained after 90 min of the experiment was recorded. The custom-built setup is shown in Figure 6. We used the temperature of 60 °C because a previous study determined 60 °C as the temperature to which a fuel surface is cooled within a few seconds of foam application.[60] We kept the oven volume at the same temperature to avoid any condensation. This model experiment allows observation of the behavior of a foam or

https://doi.org/10.1021/acsami.3c10228
ACS Appl. Mater. Interfaces 2023, 15, 49749−49761

suspension after application to a fire, and the less fuel vapor the foam or suspension allows through its structure, the better the firefighting performance of the material.[19]

Hexane, with a boiling point of 68.7 °C,[61] was used in this experiment because of its high volatility at 60 °C. A ∼1 cm layer of suspension or foam was deposited onto the preheated (60 °C) hexane pool for each test. Only suspensions containing siloxane were used in this part of our study. Thus, in the sealing experiment, we compared the behaviors of the following materials: GB-0-s, GB-GL-s, GB-GH-s, and AFFF foam. GB-0-s and GB-GH-s did not cover the perimeter of the hexane pool when deposited; therefore, we used a spatula to push the suspension to cover the pool fully. GB-GL-s was the only GB suspension that did not require spreading assistance. This finding is consistent with our observation in the hexadecane droplet spreading experiment, where GB-GL-s was the only suspension to completely spread over the hexadecane surface.

Figure 7 shows the obtained results. Generally, we found that the GB-GL-s suspension has the best vapor sealing performance among all suspensions tested here and, therefore, has the potential to be effective in suppressing a class-B pool fire. One can see that the 1 cm layer of AFFF allowed a high amount of hexane evaporation and degraded completely (high water drainage, Figure 7e) after approximately 20 min (Figure 7c). GB-0-s (Figure 7a) also allowed a high amount of hexane evaporation, especially within the 0−20 and 70−90 min time frames, yet GB-0-s drained the least amount of water of the suspensions in this experiment. The majority of the lost water evaporated from the suspension. As the water evaporated, the GB-0 suspension initially increased in density and sealed the hexane vapor better. However, as more water was lost, the hexane broke through the interparticle space. The GB-GH-s composition (Figure 7b) resisted hexane diffusion for the first 40 min, but between 40 and 90 min allowed a large amount of evaporation. We associate this observation with significant water loss via drainage by this suspension. It is suggested that GB-GH-s experienced more drainage than GB-GL-s/GB-0 because GB-GH-s contained more free water in the suspension with a high concentration of surfactant rejected by the brush grafted. Since siloxane has an affinity to hydrocarbons at elevated temperatures[62] the surfactant carries the water through the water/hexane boundary. GB-GL-s demonstrated relatively low drainage, with the most water lost via evaporation; see Figure 7b. Thus, as water evaporates/drains, the suspension densifies without losing much water from the swollen grafted layer, effectively preventing the hexane evaporation.

Fire Extinguishment with the Glass Bubble Suspensions. The final experiment we conducted was a benchtop fire extinguishment test. As a benchmark for a nonfluorinated fire extinguishing system containing siloxane, we use a composition developed by the NRL.[9,18,19,23,24,26,50] We used heptane to compare our results with the findings in previous studies of fire extinguishment with AFFF and NRL foams.[49] Also, heptane is one of the main components of gasoline and is the fuel used in UL-162, a class-B firefighting agent standard test.[63] Our experiment design is shown in Figure 8. This experiment was conducted under a fume hood. In each test, we allowed the heptane fire to burn for 60 s before depositing a foam or suspension. The temperature of the fire was consistently 125−155 °C. The highest temperatures measured were between 190 and 220 C, but the temperature only got that high sporadically. The results of these tests are shown in Figure 9 and 10. We used the 70 mL/min rate for the firefighting foams, which is 35 L/m^2/min, because this was the lowest flow rate possible in our experimental setup. We used a peristaltic pump to dispense the GB suspensions onto a heptane fire. The peristaltic pump was calibrated to 70 mL/min using water, but after the tests were conducted, we discovered the dispensing rate for the GB suspensions was 61 mL/min, which is 30.5 L/m^2/min. The videos of these experiments are shown in the Supporting Information (Videos S6−S10).

The extinguishment times of AFFF and the NRL composition at 35 L/m^2/min shown in Figure 9a agree with those of Ananth et al.[9] We found that as expected, the GB-GL-s composition extinguished the heptane fire most efficiently out of the GB-based suspensions. GB-GL-s also covered the heptane pool the fastest out of all of the GB suspensions. Since the dispensing rate of the foam system was higher than that of the GB suspensions, we calculated the volume required of each material to extinguish the fire (Figure 9b). One can see that GB-GL-s is somewhat superior to the NRL composition and only 10% below AFFF in firefighting ability. We found a strong correlation between the time a suspension takes to cover the fuel surface and the extinguishing time of the material (Figure 9c). The results from the spreading and sealing experiments for the GB suspensions agree with the fire extinguishment results. GB-GL-s displayed the best sealing ability in that it allowed the least amount of hexane evaporation, and GB-GL-s also showed the lowest extinguishment time out of the GB suspensions.

It is worth noting that the mechanism of fire extinguishment of GB-0-s is different from that of GB-GL-s and GB-GH-s. GB-0-s, when applied to a fire, does not completely cover the heptane surface. Instead, heptane is forced upward along the wall of the beaker as more suspension is applied, and the fire is extinguished only when capillary action is insufficient to feed the fire and the suspension reaches the top of the beaker. This is evident from the images presented in Figure 10. Conversely, GB-GL-s and GB-GH-s appeared to seal the heptane surface when applied.

Further, following each fire extinguishment test, we collected the GB suspension applied to the fire, rinsed, dried, and reused the GBs for subsequent fire tests. We reused each batch of GBs in the fire extinguishment test a minimum of three times and did not see any degradation in their properties or performance. Therefore, the suspensions can be collected and reused after application to a fire, which is a capability that no liquid foam or dry chemical possesses.

Burnback Test. A burnback test is normally conducted on firefighting foams to measure their resistance to the reignition of fire following extinguishment. We could not conduct a traditional burnback test wherein a small pool of burning fuel in a pot with an area of roughly 3% of the area of the large pan is lowered into the foam after the fire has been extinguished.[64,65] In this traditional test, the time for 25% of the pan to ignite is measured (or the entire pan in smaller setups). Since our beaker was only 5 cm in diameter, we were not able to conduct the burnback test in a traditional manner. Instead, to show the difference in burnback performance of liquid firefighting foams and our GB suspensions, we heated the foams and suspensions directly with a propane torch. From doing so, we observed the AFFF and NRL compositions degrade within less than a minute, exposing the bare fuel surface. However, all GB suspensions were very stable in the presence of the torch, and we observed no reignition of the

https://doi.org/10.1021/acsami.3c10228
ACS Appl. Mater. Interfaces 2023, 15, 49749−49761

heptane pool. The videos of these experiments are shown in the Supporting Information (Videos S11–S14).

CONCLUSIONS

In this work, we demonstrated that aqueous suspensions of GBs, in principle, can be used to extinguish hydrocarbon pool fires. GB-GL, the GB system with a grafted POEGMA layer of higher molecular weight and lower grafting density, proved superior to the more densely grafted GB-GH and nongrafted GB-0 system. To this end, the GB-GL suspension displayed a less negative spreading coefficient and lower viscosity than the GB-GH/GB-0 compositions. When a siloxane surfactant was added to all GB suspensions, the interfacial properties were dominated by the surfactant, with all suspensions now having the same positive spreading coefficient. However, the viscosity of the suspension containing siloxane GB-GL-s was the lowest among those studied here. The low viscosity of the GB-GL-based compositions is due to its thick, water-swollen polymer shell, which provides lubrication and repulsion between the glass bubbles. As such, this suspension demonstrated the most efficient spreading over model hydrocarbon solid (polyethylene) and liquid (hexadecane) surfaces, as well as retardation of hexane evaporation when placed over the heated hexane pool.

Finally, we used the GB suspensions and two traditional liquid firefighting foams to extinguish heptane pool fires. GB-GL-s was the most efficient GB suspension in extinguishing the fire due to its spreading and sealing ability. GB-GL-s was within 10% of the fire extinguishment performance of AFFF. The advantages of GB-GL-s over AFFF, however, are that GB-GL-s: (1) uses environmentally friendly materials, (2) offers the ability to "apply and forget" as the pool fire will not reignite, even with a torch applied to the suspension, and (3) can be collected and reused following fire extinguishment.

ASSOCIATED CONTENT

Supporting Information

The Supporting Information is available free of charge at https://pubs.acs.org/doi/10.1021/acsami.3c10228.

Videos of suspensions spreading over the hexadecane pool and fire extinguishing and burnback experiments; preparation of the grafted glass bubbles; characterization of the glass bubbles; polymer characterization; preparation of the glass bubble suspensions; surface and interfacial tension measurements; viscosity measurements; spreading measurements; UV-Vis measurements; sealing measurements; and heptane fire extinguishment test (PDF)

(MP4)

(MP4)

(MP4)

(MP4)

(MOV)

(MOV)

(MOV)

(MOV)

(MP4)

(MP4)

(MOV)

(MOV)

(MOV)

(MOV)

AUTHOR INFORMATION

Corresponding Author

Igor Luzinov − *Department of Materials Science and Engineering, Clemson University, Clemson, South Carolina 29634, United States;* orcid.org/0000-0002-1604-6519; Email: luzinov@clemson.edu

Authors

Randall T. Snipes − *Department of Materials Science and Engineering, Clemson University, Clemson, South Carolina 29634, United States*

Mauricio Melara − *Department of Materials Science and Engineering, Clemson University, Clemson, South Carolina 29634, United States*

Andrii Tiiara − *Department of Materials Science and Engineering, Clemson University, Clemson, South Carolina 29634, United States*

Jeffery Owens − *Air Force Civil Engineer Center, Tyndall AFB, Panama City, Florida 32403, United States*

Complete contact information is available at: https://pubs.acs.org/10.1021/acsami.3c10228

Notes

The authors declare no competing financial interest.

ACKNOWLEDGMENTS

The research reported was partially supported by the US Air Force Civil Engineer Center via ORISE (Oak Ridge Institute for Science and Education) program and the National Science Foundation via EPSCoR OIA-1655740. The authors thank (i) Artis Brasovs, Yueming Sun, and Konstantine Kornev (Clemson University) for fruitful discussions and help with surface tension and viscosity measurements; (ii) Kim Ivey (Clemson University) for help with TGA measurements; (iii) Mohammad Aghajohari and Sergiy Minko (University of Georgia) for fruitful discussions and help with light scattering measurements.

REFERENCES

(1) Hinnant, K. M.; Ananth, R.; Farley, J. P.; Whitehurst, C. L.; Giles, S. L.; Maza, W. A.; Snow, A. W.; Karwoski, S.; Hughes, J. Extinction Performance Summary of Commercial Fluorine-free Firefighting Foams over a 28 ft2 Pool Fire Detailed by MIL-PRF-24385; Naval Research Lab Washington: DC Washington, United States, https://apps.dtic.mil/sti/pdfs/AD1100426.pdf, 2020. Accessed 9/29/2023

(2) https://www.nationalgeographic.com/science/2020/01/pfas-contamination-safe-drinking-water-study/ (accessed July 12, 2023).

(3) Guo, J.; Resnick, P.; Efimenko, K.; Genzer, J.; DeSimone, J. M. Alternative Fluoropolymers to Avoid the Challenges Associated with Perfluorooctanoic Acid. *Ind. Eng. Chem. Res.* **2008**, *47* (3), 502−508.

(4) Conder, J. M.; Hoke, R. A.; Wolf, W. d.; Russell, M. H.; Buck, R. C. Are PFCAs Bioaccumulative? A Critical Review and Comparison with Regulatory Criteria and Persistent Lipophilic Compounds. *Environ. Sci. Technol.* **2008**, *42* (4), 995−1003.

(5) US Environmental Protection Agency: Long-chain perfluorinated chemicals (PFCs) action plan. https://www.epa.gov/assessing-and-managing-chemicals-under-tsca/long-chain-perfluorinated-chemicals-pfcs-action-plan (accessed July 12, 2023).

(6) Buck, R. C.; Franklin, J.; Berger, U.; Conder, J. M.; Cousins, I. T.; de Voogt, P.; Jensen, A. A.; Kannan, K.; Mabury, S. A.; van Leeuwen, S. P. J. Perfluoroalkyl and Polyfluoroalkyl Substances in the Environment: Terminology, Classification, and Origins. *Integr. Environ. Asses.* **2011**, *7* (4), 513−541.

(7) Moody, C. A.; Field, J. A. Perfluorinated Surfactants and the Environmental Implications of Their Use in Fire-Fighting Foams. *Environ. Sci. Technol.* **2000**, *34* (18), 3864−3870.
(8) Horst, J.; Quinnan, J.; McDonough, J.; Lang, J.; Storch, P.; Burdick, J.; Theriault, C. Transitioning Per- and Polyfluoroalkyl Substance Containing Fire Fighting Foams to New Alternatives: Evolving Methods and Best Practices to Protect the Environment. *Ground Water Monit. Remediat.* **2021**, *41* (2), 19−26.
(9) Giles, S. L.; Snow, A. W.; Hinnant, K. M.; Ananth, R. Modulation of Fluorocarbon Surfactant Diffusion with Diethylene Glycol Butyl Ether for Improved Foam Characteristics and Fire Suppression. *Colloids Surf., A* **2019**, *579*, 123660.
(10) Rosen, M. R.; Sterman, S.; Schwarz, E. G. Method of extinguishing liquid hydrocarbon fires and composition therefor comprising silicone surfactants. U.S. Patent 3,621,917 A, Nov 23, 1971.
(11) Rosen, M. R.; Pokai, B. Method of extinguishing fires and compositions therefor containing cationic silicone surfactants. U.S. Patent 3,677,347 A, July 18, 1972.
(12) Chelsea, P. J. Fire fighting. U.S. Patent 3,957,657 A, May 18, 1976.
(13) Blunk, D.; Hetzer, R. H.; Sager-Wiedmann, A.; Wirz, K. Siloxane-containing fire extinguishing foam. U.S. Patent 9,446,272 B2, Sept 20, 2016.
(14) Hetzer, R.; Kümmerlen, F.; Wirz, K.; Blunk, D.; Blunk, D. Fire Testing a New Fluorine-free AFFF Based on a Novel Class of Environmentally Sound High Performance Siloxane Surfactants. *Fire Saf. Sci.* **2014**, *11*, 1261−1270.
(15) Wang, P. Application of Green Surfactants Developing Environment Friendly Foam Extinguishing Agent. *Fire Technol.* **2015**, *51* (3), 503−511.
(16) Pabon, M.; Corpart, J. M. Fluorinated Surfactants: Synthesis, Properties, Effluent Treatment. *J. Fluorine Chem.* **2002**, *114* (2), 149−156.
(17) Martin, T. J. Fire-Fighting Foam Technology. In *Foam Engineering: Fundamentals and Applications*; Stevenson, P., Ed.; John Wiley & Sons: Hoboken, 2012; pp 411−457.
(18) Hinnant, K. M.; Giles, S. L.; Ananth, R. Measuring Fuel Transport Through Fluorocarbon and Fluorine-Free Firefighting Foams. *Fire Saf. J.* **2017**, *91*, 653−661.
(19) Hinnant, K.; Giles, S.; Ananth, R. Measuring Fuel Transport Through Fluorocarbon and Fluorine-Free Firefighting Foams. *Fire Saf. J.* **2017**, *91*, 653−661.
(20) Harkins, W. D.; Feldman, A. Films. The Spreading of Liquids and the Spreading Coefficient. *J. Am. Chem. Soc.* **1922**, *44* (12), 2665−2685.
(21) Lattimer, B. Y.; Trelles, J. Foam Spread Over a Liquid Pool. *Fire Saf. J.* **2007**, *42* (4), 249−264.
(22) Aksoy, Y. T.; Eneren, P.; Koos, E.; Vetrano, M. R. Spreading of a Droplet Impacting on a Smooth Flat Surface: How Liquid Viscosity Influences the Maximum Spreading Time and Spreading Ratio. *Phys. Fluids* **2022**, *34* (4), 042106.
(23) Hinnant, K.; Ananth, R.; Conroy, M.; Williams, B. Evaluating Differences in Foam Degradation Between Perfluoroalkyl and Fluorine-Free Foams for the Development of Environmentally Friendly Firefighting Alternatives. *Abstracts of Papers of the American Chemical Society*: San Diego, 2016; Vol. *251*, p ENVR 131.
(24) Hinnant, K.; Giles, S.; Smith, E.; Snow, A.; Ananth, R. Characterizing the Role of Fluorocarbon and Hydrocarbon Surfactants in Firefighting-Foam Formulations for Fire-Suppression. *Fire Technol.* **2020**, *56*, 1413−1441.
(25) Hinnant, K. M.; Conroy, M. W.; Ananth, R. Influence of Fuel on Foam Degradation for Fluorinated and Fluorine-Free Foams. *Colloids Surf., A* **2017**, *522*, 1−17.
(26) Henze, M.; Mädge, D.; Prucker, O.; Rühe, J. Grafting Through": Mechanistic Aspects of Radical Polymerization Reactions with Surface-Attached Monomers. *Macromolecules* **2014**, *47* (9), 2929−2937.
(27) Tsubokawa, N.; Kogure, A.; Maruyama, K.; Sone, Y.; Shimomura, M. Graft Polymerization of Vinyl Monomers from Inorganic Ultrafine Particles Initiated by Azo Groups Introduced onto the Surface. *Polym. J.* **1990**, *22* (9), 827−833.
(28) Budov, V. Hollow glass microspheres. use, properties, and technology (Review). *Glass Ceram.* **1994**, *51* (7−8), 230−235.
(29) Li, D.; Sheng, X.; Zhao, B. Environmentally Responsive "Hairy" Nanoparticles: Mixed Homopolymer Brushes on Silica Nanoparticles Synthesized by Living Radical Polymerization Techniques. *J. Am. Chem. Soc.* **2005**, *127* (17), 6248−6256.
(30) Prucker, O.; Rühe, J. Mechanism of Radical Chain Polymerizations Initiated by Azo Compounds Covalently Bound to the Surface of Spherical Particles. *Macromolecules* **1998**, *31* (3), 602−613.
(31) Prucker, O.; Rühe, J. Synthesis of Poly(styrene) Monolayers Attached to High Surface Area Silica Gels through Self-Assembled Monolayers of Azo Initiators. *Macromolecules* **1998**, *31* (3), 592−601.
(32) Iyer, K. S.; Luzinov, I. Effect of Macromolecular Anchoring Layer Thickness and Molecular Weight on Polymer Grafting. *Macromolecules* **2004**, *37* (25), 9538−9545.
(33) Sperling, L. H. *Introduction to Physical Polymer Science*, 4th ed.; Wiley-Interscience: Hoboken, NJ, 2006; p 845.
(34) Hiemenz, P. C.; Lodge, T. *Polymer Chemistry*, 2nd ed.; CRC Press: Boca Raton, 2007; p 587.
(35) Rubinstein, M.; Colby, R. H. *Polymer Physics*; Oxford University Press: Oxford, 2003; p 442.
(36) Zhao, B.; Brittain, W. J. Polymer Brushes: Surface-Immobilized Macromolecules. *Prog. Polym. Sci.* **2000**, *25* (5), 677−710.
(37) Zdyrko, B.; Luzinov, I. Polymer Brushes by the "Grafting to" Method. *Macromol. Rapid Commun.* **2011**, *32* (12), 859−869.
(38) Samadi, A.; Husson, S. M.; Liu, Y.; Luzinov, I.; Michael Kilbey, S. Low-Temperature Growth of Thick Polystyrene Brushes via ATRP. *Macromol. Rapid Commun.* **2005**, *26* (23), 1829−1834.
(39) Chen, W.-L.; Cordero, R.; Tran, H.; Ober, C. K. 50th Anniversary Perspective: Polymer Brushes: Novel Surfaces for Future Materials. *Macromolecules* **2017**, *50* (11), 4089−4113.
(40) Zhang, N.; Huber, S.; Schulz, A.; Luxenhofer, R.; Jordan, R. Cylindrical Molecular Brushes of Poly (2-oxazoline) s from 2-Isopropenyl-2-oxazoline. *Macromolecules* **2009**, *42* (6), 2215−2221.
(41) Panyukov, S.; Zhulina, E. B.; Sheiko, S. S.; Randall, G. C.; Brock, J.; Rubinstein, M. Tension Amplification in Molecular Brushes in Solutions and on Substrates. *J. Phys. Chem. B* **2009**, *113* (12), 3750−3768.
(42) Rzayev, J. Molecular Bottlebrushes: New Opportunities in Nanomaterials Fabrication. *ACS Macro Lett.* **2012**, *1* (9), 1146−1149.
(43) Tu, S. D.; Choudhury, C. K.; Luzinov, I.; Kuksenok, O. Recent Advances Towards Applications of Molecular Bottlebrushes and their Conjugates. *Curr. Opin. Solid State Mater. Sci.* **2019**, *23* (1), 50−61.
(44) Verduzco, R.; Li, X. Y.; Pesek, S. L.; Stein, G. E. Correction: Structure, function, self-assembly, and applications of bottlebrush copolymers. *Chem. Soc. Rev.* **2015**, *44* (21), 7916.
(45) Wintermantel, M.; Gerle, M.; Fischer, K.; Schmidt, M.; Wataoka, I.; Urakawa, H.; Kajiwara, K.; Tsukahara, Y. Molecular Bottlebrushes. *Macromolecules* **1996**, *29* (3), 978−983.
(46) Sheiko, S. S.; Panyukov, S.; Rubinstein, M. Bond Tension in Tethered Macromolecules. *Macromolecules* **2011**, *44* (11), 4520−4529.
(47) Vanderwerff, J. C.; Dekruif, C. G. Hard-Sphere Colloidal Dispersions - The Scaling of Rheological Properties with Particle-Size, Volume Fraction, and Shear Rate. *J. Rheol.* **1989**, *33* (3), 421−454.
(48) Shinoda, K.; Hato, M.; Hayashi, T. Physicochemical Properties of Aqueous-Solutions of Fluorinated Surfactants. *J. Phys. Chem.* **1972**, *76* (6), 909−914.
(49) Ananth, R.; Snow, A. W.; Hinnant, K. M.; Giles, S. L.; Farley, J. P. Synergisms Between Siloxane-Polyoxyethylene and Alkyl Polyglycoside Surfactants in Foam Stability and Pool Fire Extinction. *Colloids Surf., A* **2019**, *579*, 123686.
(50) Ananthapadmanabhan, K. P.; Goddard, E. D.; Chandar, P. A Study of the Solution, Interfacial and Wetting Properties of Silicone Surfactants. *Colloids Surf.* **1990**, *44*, 281−297.

https://doi.org/10.1021/acsami.3c10228
ACS Appl. Mater. Interfaces 2023, 15, 49749−49761

(51) Anton Paar. The influence of particles on suspension rheology. https://wiki.anton-paar.com/nl-en/the-influence-of-particles-on-suspension-rheology/ (accessed July 12, 2023).
(52) Wagner, N. J.; Brady, J. F. Shear Thickening in Colloidal Dispersions. *Phys. Today* **2009**, *62* (10), 27−32.
(53) Ploehn, H. J.; Goodwin, J. W. Rheology of Aqueous Suspensions of Polystyrene Latex Stabilized by Grafted Poly(Ethylene Oxide). *Faraday Discuss.* **1990**, *90*, 77−90.
(54) Israelachvili, J. N. *Intermolecular and Surface Forces*; Academic Press: London, 1991.
(55) Soni, S. S.; Sastry, N. V.; Aswal, V. K.; Goyal, P. S. Micellar Structure of Silicone Surfactants in Water from Surface Activity, SANS and Viscosity Studies. *J. Phys. Chem. B* **2002**, *106* (10), 2606−2617.
(56) Krieger, I. M.; Dougherty, T. J. A Mechanism for Non-Newtonian Flow in Suspensions of Rigid Spheres. *Trans. Soc. Rheol.* **1959**, *3* (1), 137−152.
(57) Mark, J. E. *Polymer Data Handbook*; Oxford University Press, 2009.
(58) Rolo, L. I.; Caço, A. I.; Queimada, A. J.; Marrucho, I. M.; Coutinho, J. A. P. Surface Tension of Heptane, Decane, Hexadecane, Eicosane, and Some of Their Binary Mixtures. *J. Chem. Eng. Data* **2002**, *47* (6), 1442−1445.
(59) Riddick, J. A.; Bunger, W. B.; Sakano, T. K. *Organic Solvents: Physical Properties and Methods of Purification*. 4th ed.; John Wiley and Sons: New York, NY, United States, 1986.
(60) Conroy, M. W.; Fleming, J. W.; Ananth, R. Surface Cooling of a Pool Fire by Aqueous Foams. *Combust. Sci. Technol.* **2017**, *189* (5), 806−840.
(61) Tongberg, C.; Johnston, F. Vapor-Liquid Equilibria for N-hexane—Benzene Mixtures. *Ind.Eng.Chem.* **1933**, *25* (7), 733−735.
(62) Banerjee, A.; Liu, Y. H. Essential Factor of Perfluoroalkyl Surfactants Contributing to Efficacy in Firefighting Foams. *Langmuir* **2021**, *37* (30), 8937−8944.
(63) https://www.firefightingfoam.com/knowledge-base/international-standards/ul-162/ (accessed July 12, 2023).
(64) Performance specification, fire extinguishing agent, fluorine-free foam (F3) liquid concentrate for land-based, fresh water applications. Mil-Spec MIL-PRF-32725, (6 January 2023). https://media.defense.gov/2023/Jan/12/2003144157/-1/-1/1/MILITARY-SPECIFICATION-FOR-FIRE-EXTINGUISHING-AGENT-FLUORINE-FREE-FOAM-F3-LIQUID-CONCENTRATE-FOR-LAND-BASED-FRESH-WATER-APPLICATIONS.PDF (accessed July 12, 2023).
(65) Performance Specification, Fire Extinguishing Agent, Aqueous Film -Forming Foam (AFFF) Liquid Concentrate, For Fresh and Sea Water Mil-Spec MIL-PRF-24385F(SH), w/INT. AMENDMENT 4, (7 April 2020). https://www.firefightingfoam.com/knowledge-base/international-standards/mil-f-24385/#:~:text=MIL%2DF%2D24385isa,expensivetesttohavedone! (accessed July 12, 2023).

https://doi.org/10.1021/acsami.3c10228
ACS Appl. Mater. Interfaces 2023, 15, 49749−49761